Time Development of the Flow about an Impulsively Started Cylinder

F. D. Deffenbaugh*
TRW Systems, Redondo Beach, Calif.
and
F. J. Marshall†
Purdue University, West Lafayette, Ind.

A method is developed to determine the time-dependent flowfield about an impulsively started circular cylinder. An outer potential flow model is interfaced with an inner viscous flow region. The wake is described by a set of elementary point vortices. The position at which the point vortices are shed from the cylinder is obtained from a solution to the unsteady incompressible laminar boundary-layer equations. A rear shear-layer is postulated to account for backflow induced vorticity. Wake development is detailed from the initial formation of the two symmetric vortices to subsequent asymmetry and eventual alternate shedding. Unsteady pressure distributions, lift and drag forces, and Strouhal number are calculated and compared with experiment.

Nomenclature

a = cylinder radius
C_D = coefficient of drag, $2D/\rho U^2$
C_{ds} = coefficient of drag due to shear
C_L = coefficient of lift, $2L/\rho U^2$
$(\bar{C}_L^2)^{1/2}$ = root mean square lift coefficient
C_p = coefficient of pressure, $2(p-p_\infty)/\rho U^2$
d = cylinder diameter
D = drag
$H(t)$ = step function ($=0$, $t\leq 0$; $=1$, $t>0$)
L = lift
m = location of vortex born from boundary layer – rear shear layer
p = pressure
r = polar radius
r_c = vortex core
Re = Reynolds number, Ud/ν
t = nondimensional time, Ut^*/a
Δt = numerical stepsize
U = freestream velocity
$(\tilde{u},\tilde{v})$ = cartesian velocity components
(u,v) = polar velocity components
w = complex velocity potential, $\Phi+i\Psi$
θ = polar angle
ν = kinematic viscosity
ρ = density
Γ = circulation
Φ = potential function
Ψ = stream function
ω = vorticity

Subscripts and Superscripts

$(\,)^*$ = dimensional
$(\,)^\circ$ = outer flow
$(\,)_\circ^\circ$ = outer flow evaluated at surface
$\bar{(\,)}$ = inner flow
$\hat{(\,)}$ = lower half of cylinder
$(\,)^f$ = forward
$(\,)^r$ = rear
$(\,)_m$ = extremum
$(\,)_s$ = separation point
$(\,)_k$ = at time t_k
$(\,)_n$ = point vortex n
$(\,)_0$ = stagnation point
$(\,)_{,r}$ = partial derivatives
$(\,)_{,\theta}$ = partial derivatives
$(\,)_{,t}$ = partial derivatives

Received May 9, 1975; revision received Feb. 17, 1976. This work was partially supported by NASA Grant NGR15-005-119 and has been carried out in partial fulfillment of the requirements for the degree of Doctor of Philosophy of the School of Aeronautics and Astronautics, Purdue University.

Index categories; Nonsteady Aerodynamics; Jets, Wakes, and Viscid-Inviscid Flow Interactions; Boundary Layers and Convective Heat Transfer – Laminar.

*Member of the Professional Staff. Member AIAA.

†Professor, School of Aeronautics and Astronautics. Member AIAA.

Introduction

THE time development of flow about an impulsively started circular cylinder is a classic problem in fluid mechanics. The combination of simple geometry, complicated flow phenomena, and flow interaction has led to extensive study by both experimental and theoretical investigators.

In the past, two basic theoretical approaches have been used to determine the flowfield about an impulsively started circular cylinder: 1) a finite-difference solution to the full Navier-Stokes equations, and 2) an approximate potential flow model. Payne[1] developed the first finite-difference solution for symmetric flow at Reynolds numbers 40 and 100; Kawaguti and Jain[2] extended this range from 1-100. Thoman and Szewczyk[3] developed a solution for asymmetric flow for Reynolds number $1\text{-}3\times10^4$. In the second approach, potential flow models exist ranging from the work of Mello[4] and Bryson,[5] in which the potential flow is modified by two symmetric vortices placed in the wake behind the cylinder, to the more complicated models of Gerrard[6] and Sarpkaya,[7] in which the shear layers shed from the cylinder are modeled by point vortices as proposed by Abernathy and Kronauer.[8]

This study extends the potential flow model to include viscous effects. The time development of the flowfield about a circular cylinder started impulsively from rest is described by interfacing an inner boundary-layer solution with an outer potential discrete point vortex wake solution. The dynamic interaction between the discrete point vortex wake and boundary-layer separation provides physical insight to the mechanism of the creation, growth, and eventual alternate shedding of the vortices behind bluff bodies.

General Solution Technique

The Reynolds number range considered is the high-laminar regime ($10^4<Re<10^5$). The technique assumes that for a

high Reynolds number the flow may be divided into two regions: a viscous inner flow near the cylinder described by a boundary layer and a rear shear layer and an essentially inviscid outer flow elsewhere. Computer solutions for these subflowfields are matched based on the physics of the problem. This technique involves no finite differences and is the potential flow model approach with one basic difference; i.e., the inner viscous solution (a solution to the boundary-layer equations and rear shear layer) determines the position at which the point vortices are to be placed into the flow.

Outer Flow

The outer flow consists of an irrotational flow outside the boundary layer and rear shear layer, and a wake. The flow is assumed to be a potential flow consisting of the superposition of vortex, uniform flow, and doublet (the classical potential flow about a cylinder with circulation), plus the potential flow induced by a set of point vortices located outside the cylinder and their images inside.

In terms of the nondimensional quantities $(x,y,t)=(x^*/a,\ y^*/a,\ Ut^*/a)$, $(r,\theta)=(r^*/a,\ \theta)$, $\Phi+i\Psi=(\Phi^*+i\Psi^*)/Ua$, $\omega=\omega^* a/U$, $\Gamma=\Gamma^*/Ua$, the equations for the outer flow are

$$\text{D.E.} \quad \nabla^2\Psi=\omega \tag{1}$$

$$\text{I.C.} \quad t=0\ ;\ \Psi=0 \tag{2}$$

$$\text{B.C.} \quad r=1\ ;\ \Psi=0$$

$$r\to\infty\ ;\Psi=yH(t),\quad H(t)=0\ \ t\le 0$$

$$H(t)=1\ \ t>0 \tag{3}$$

where

$$\omega(x,y,t)=\sum_{n=1}^{N}\Gamma_n\delta(x-x_n)\delta(y-y_n)$$

The (x_n,y_n) represent the location of a point vortex, Γ_n is the vortex strength, and δ is the delta function such that upon integrating overall x,y external to the cylinder,

$$\int\int \omega\,dS=\sum_{n=1}^{N}\Gamma_n$$

The solution obtained using the Circle Theorem[9] is

$$w=\Phi+i\Psi=z+\frac{1}{z}+\frac{i\Gamma_0}{2\pi}\log z + \sum_{n=1}^{N}\frac{i\Gamma_n}{2\pi}\log\frac{(z-z_n)z}{\left(z-\dfrac{z_n}{|z_n|^2}\right)z_n} \tag{4}$$

where

$$z=x+iy=re^{i\theta} \tag{5a}$$

$$z_n=x_n+iy_n=\ell_n e^{i\theta n} \tag{5b}$$

$$z-z_n=(x-x_n)+i(y-y_n)=r_{1n}e^{i\theta 1n} \tag{5c}$$

$$z-\frac{z_n}{|z_n|^2}=\left(x-\frac{x_n}{\ell_n^2}\right)+i\left(y-\frac{y_n}{\ell_n^2}\right)=r_{2n}e^{i\theta 2n} \tag{5d}$$

such that on the surface $r_{2n}=r_{1n}/\ell_n$ and $\Psi=0$. The cartesian components of velocity $(\bar{u},\bar{v})$ and the tangential and radial velocity components (u,v) can be obtained from Eq. (4) as

$$dw/dz=-\bar{u}+i\bar{v}=e^{-i\theta}(-v+iu) \tag{6}$$

Inner Flow

The equations for unsteady two-dimensional boundary layers in laminar incompressible flow, nondimensionalized as in the outer flow, and written in polar coordinates are

$$\bar{u}_{,t}+\bar{u}\bar{u}_{,\theta}+\bar{v}\bar{u}_{,\bar{r}}=-p_{,\theta}/2+\bar{u}_{,\bar{r}\bar{r}} \tag{7}$$

$$0=p_{,\bar{r}} \tag{8}$$

$$\bar{u}_{,\theta}+\bar{v}_{,\bar{r}}=0 \tag{9}$$

Evaluating $-p_{,\theta}/2$ as $\bar{r}\to\infty$, substituting the result into Eq. (7), and applying the appropriate initial and boundary conditions yields the governing equations for the inner flow; i.e.,

$$\bar{u}_{,t}+\bar{u}\bar{u}_{,\theta}+\bar{v}\bar{u}_{,\bar{r}}=u_o^o{}_{,t}+u_o^o\,u_{o,\theta}^o+\bar{u}_{,\bar{r}\bar{r}} \tag{10}$$

$$\bar{u}_{,\theta}+\bar{v}_{,\bar{r}}=0 \tag{11}$$

$$\text{I.C.} \quad t=0\ ;\ \bar{u}=\bar{v}=0 \tag{12}$$

$$\text{B.C.} \quad \bar{r}=1\ ;\ \bar{u}=\bar{v}=0$$

$$\bar{r}\to\infty\ ;\ \bar{u}=u_o^o(\theta,t) \tag{13}$$

where $(\ )_o^o$ denotes the evaluation of the outer flow at the surface. Equations (10-13) are solved by an approximate method based on the integral form of the momentum equations. The method is basically that of Schuh's[10] with the modification that the outer potential flow is time dependent, thus requiring a numerical integration of Schuh's basic equations.

Shortly after impulsive start the inner boundary-layer solution closely approaches the steady state even through the outer flow is continually changing. For times where the boundary layer is nearly steady, the effect of the unsteady outer flow is handled using a quasi-steady approximation; the time-derivative terms in Eq. (10) are dropped and Pohlhausen's[11] method is used to solve the steady boundary-layer equations. The boundary conditions at any instant in time are given by the outer potential flow solution at that time.

Prandtl's definition of separation $(\bar{u}_{,\bar{r}}=0,\bar{r}=0)$ was used to determine the boundary-layer separation point. For the early flow development, $t<1.0$, where an unsteady separation criterion might be used, the wake has not become a dominant part of the flowfield. For later times, when the boundary layer is close to steady state, quasi-steady flow and steady separation are assumed. Because the boundary layer approaches steady state very rapidly, i.e., $t=1.0$, and the separation angle during this time moves rapidly forward in a monotonic manner, use of the steady separation criterion should not introduce significant errors for long-time, steady-state solutions.

Rear Shear Layer

The primary effect of viscosity is the creation of vorticity over the cylinder surface. The vorticity created in the boundary layer is shed into the wake at the boundary-layer separation points and rolls up to form regions of concentrated vorticity immediately behind the cylinder. These vortex structures induce a backflow velocity on the rear portion of the cylinder, and vorticity of opposite sign to that created in the boundary layer is shed into the wake.

To account for this secondary source of vorticity, the existence of a rear shear layer is postulated. It is assumed that the rear shear layer is similar to a boundary layer, cannot tolerate much of an adverse pressure gradient, and separates soon after minimum backflow pressure is reached. The distance at which rear shear layer separation occurs is assumed to be proportional to the distance at which boundary layer separation occurs after pressure minimum. The opposite signed rear vorticity is introduced into the wake at the rear

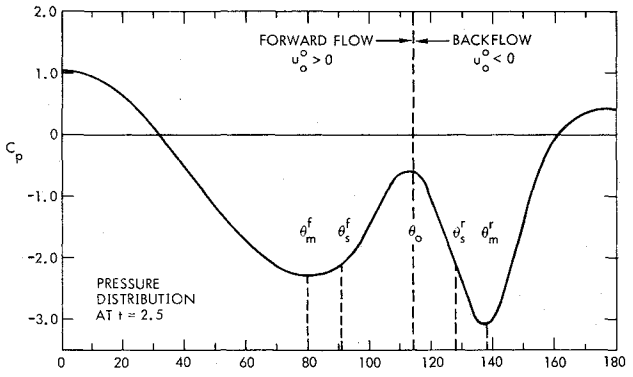

Fig. 1 Rear shear layer separation.

shear layer separation point θ_s^r, determined from the following proportional algorithm:

$$\theta_s^r - \theta_m^r = K(\theta_s^f - \theta_m^f) \tag{14}$$

where the proportionality constant $K = (\theta_0 - \theta_m^r)/(\theta_0 - \theta_m^f)$, see Fig. 1.

Interface

The prime interaction is that the outer flow drives the inner flow. The outer boundary condition on the inner flow is the outer flow evaluated at the surface; the inner flow is the source of outer flow vorticity.

The vorticity created over the forward part of the cylinder is introduced into the wake in the form of point vortices at the boundary layer separation points. The vorticity flux across the boundary layer at a separation point, θ_s, is

$$\frac{\partial \Gamma}{\partial t} = \int_0^\infty \omega u \, d\bar{r} = \int_0^\infty \frac{\partial \bar{u}}{\partial \bar{r}} \bar{u} d\bar{r} = \frac{u_o^{o2}}{2} \tag{15}$$

The vorticity flux out of the boundary layer in a time-step, Δt_k, is summed into a point vortex of strength;

$$\Gamma_n = \Delta t_k \frac{\partial \Gamma}{\partial t} \tag{16}$$

The point vortex is assumed to be in the outer potential flow and images are created simultaneously to satisfy the condition of zero normal velocity at the surface. The tangential velocity at the surface due to the newly created vortex and the corresponding images is $u_j = -\Gamma_n/\pi m$, where m is the normal distance from the cylinder at θ_s. With the requirement that the no-slip condition hold at θ_s,

$$m = \frac{|\Gamma_n|}{\pi |u_o^o|} = \frac{\Delta t_k |u_o^o|}{2\pi} \tag{17}$$

In an analogous manner, point vortices are introduced into the outer flow from the rear shear layer separation points. This is a source of vorticity of opposite sign.

The basic inviscid equations (1-3) allow for an arbitrary circulation Γ_0 determined from the viscous action. It is postulated that Γ_0 is operative only in the quasi-steady flow regime ($t \geq 4.0$) and therefore tends to equalize the vorticity production from the upper and lower separation points as

$$\Gamma_0(t_{k+1}) = \frac{-\pi}{c}\left[u_o^o(\theta_s, t_k) + u_o^o(\hat{\theta}_s, t_k)\right] \tag{18}$$

In this analysis, the overshoot factor is $c = 10$.

Wake

The wake described is a set of ideal point vortices superimposed with the classical potential flow about a cylinder. In the region of the point vortices, the fluid velocity tends to infinity. Infinite velocities are not encountered in a real fluid, and in the region of the vortex core the fluid flow cannot be considered ideal and viscosity effects must be considered. Recent studies[12,13] show that some type of artificial viscosity is required to cancel irregularities that normally occur because of the singular nature of the ideal point vortex. In this study, outside a "viscous core radius (r_c)," the velocity induced by a point vortex is the potential solution; within the core radius, the velocity is zero. The wake is thus approximated by a set of potential point vortices, with those falling within r_c of a field point ignored.

Although the inviscid wake assumption has been slightly modified by the use of an artifical viscosity in the region of the point vortices, it is assumed that the motion of the vortices is governed by the equations of inviscid flow. Hence,

$$D\omega/Dt = 0 \tag{19}$$

which implies that the point vortex strengths must remain constant in time and are constrained to move with the fluid. At each discrete step in time, t_k, a new vortex distribution is calculated at t_{k+1}; i.e.,

$$x_n(t_{k+1}) = x_n(t_k) + \tilde{u}(x_n, y_n, t_k) \cdot \Delta t_k$$
$$y_n(t_{k+1}) = y_n(t_k) + \tilde{v}(x_n, y_n, t_k) \cdot \Delta t_k \tag{20}$$

When a large number of point vortices exist in the outer flow, computation time becomes prohibitive. To reduce computer time, the vortices are coalesced, 1) to substantially reduce the number of point vortices, 2) to yield an equilvalent velocity field, and 3) to maintain the basic structure of the vortex distribution. For this operation, two point vortices of strengths Γ_1 and Γ_2 at (x_1, y_1) and (x_2, y_2), respectively, are replaced by one point vortex of strength Γ_3 at (x_3, y_3) where

$$\Gamma_3 = \Gamma_1 + \Gamma_2 \tag{21}$$

$$x_3 = \frac{(|\Gamma_1| x_1 + |\Gamma_2| x_2)}{(|\Gamma_1| + |\Gamma_2|)}, \quad y_3 = \frac{(|\Gamma_1| y_1 + |\Gamma_2| y_2)}{(|\Gamma_1| + |\Gamma_2|)} \tag{22}$$

The symmetric vortex structure is unstable at high Reynolds numbers and asymmetry develops soon after impulsive start which promotes alternate vortex shedding. The departure from the symmetric vortex configuration is assumed to be due to small experimental disturbances. To model these unknown disturbances, a perturbation is applied to the point vortex arrays at an early time arbitrarily chosen as the time the flux of vorticity out of the boundary layer is at a maximum; i.e.,

$$[\hat{x}_n(t_{k+}), \hat{y}_n(t_{k+})] = [\hat{x}_n(t_k) - 0.001, \hat{y}_n(t_k) - 0.001] \tag{23}$$

Lift and Drag

The lift and drag acting on the cylinder are calculated by integrating the pressure distribution obtained by Bernoulli's equation

$$-2\Phi_{,t} + u_o^{o2} + p = 2f(t) \tag{24}$$

The lift and drag equations in coefficient form are

$$C_L = -\frac{1}{2}\int_0^{2\pi} C_p \sin\theta \, d\theta \tag{25}$$

$$C_D = \frac{1}{2}\int_0^{2\pi} C_p \cos\theta \, d\theta \tag{26}$$

where C_p is obtained from Eqs. (4-6) and (24) as

$$C_p = 1 - u_o^{o2} - 2\sum_{n=1}^{N} \frac{\Gamma_n}{2\pi}(\dot{\theta}_{1n} - \dot{\theta}_{2n}) \tag{27}$$

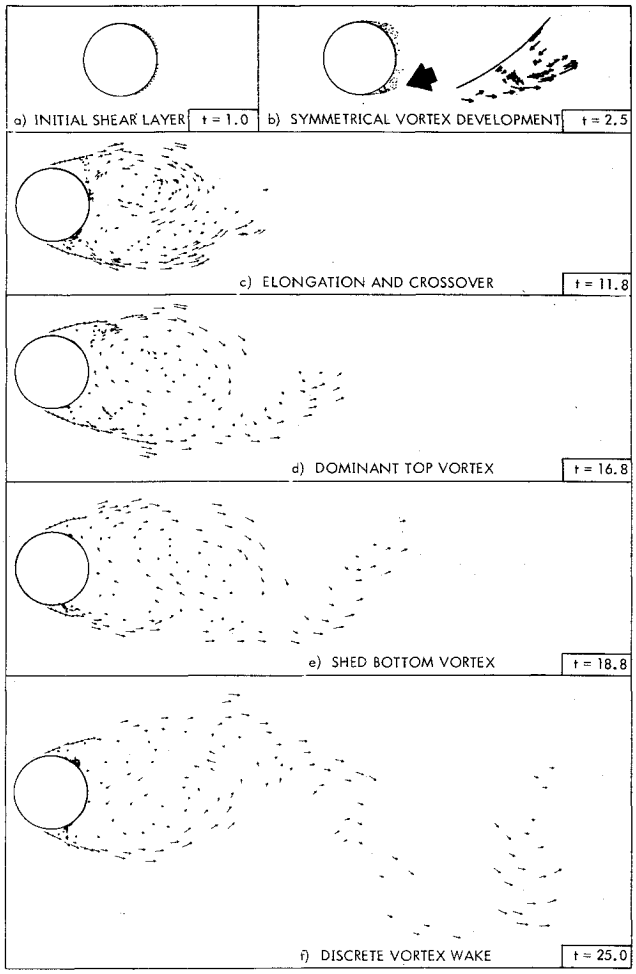

Fig. 2 Vortex wake development.

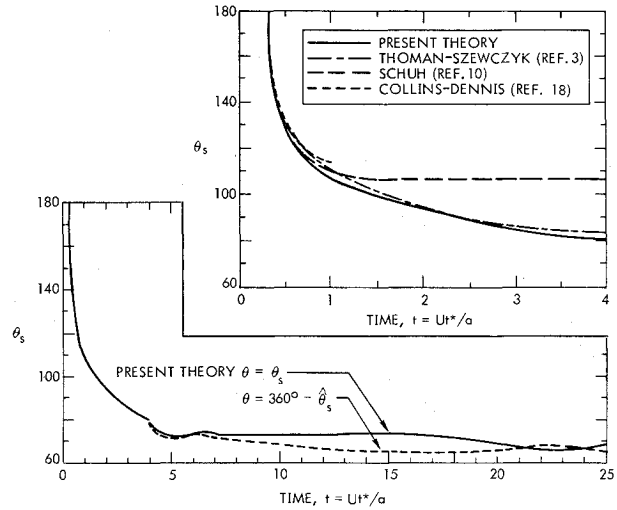

Fig. 3 Transient separation point.

For an inviscid model, the forces on a moving cylinder can be determined directly by Lagally's theorem[7,9] or by a vortex impulse method.[14] In the current mathematical model, lift and drag are obtained by integration because diffusive effects enter the primarily inviscid model through the parameter r_c. The pressure distribution around the cylinder is useful in comparing theoretical and experimental results, as well as in understanding the mechanism of vortex shedding.

Results

A direct comparison of theory to experiment is not possible for the early, transient phases of the flow because, experimentally, a finite acceleration of the cylinder from rest to a constant velocity must exist. A comparison between theory and experiment is possible when the flow becomes periodic and the drag approaches a steady value.

Vortex Capture

Several explanations exist for the vortex shedding mechanism. The explanations of Gerrard[15] and Sarpkaya[16] were based on experimental observations while those of Thoman and Szewczyk[3] were based on theoretical calculations. All agreed on the basic premise that a vortex is captured by a stream of fluid from the opposite side of the cylinder; however, the capture mechanism of the first and subsequent vortices has not been resolved.

In the present model, the point vortex distribution (with viscous core radius $r_c = 0.05$) fixes the flowfield at any instant in time through Poisson's equation, $\nabla^2\psi = \omega$. The vorticity equation, $D\omega/Dt = 0$, is used to determine the vorticity distribution at the next instant and the velocity field is calculated again. The velocity field at t_k, as well as the change in distribution of vorticity are shown in Fig. 2; the point vortices are plotted at t_k and t_{k+1} with arrows drawn between corresponding vortices at successive times. The growth and subsequent alternate shedding of large scale vortices are explained by the discrete vortex wake model.

Shortly after impulsive start, the boundary layer separates from the rear stagnation point and the separation point moves rapidly toward its final steady value (Fig. 2a). The separated shear layers begin to form two symmetric vortices behind the cylinder. The vortices immediately behind the cylinder induce high backflow velocities which create vorticity of opposite sign to the main vortices; the opposite signed vorticity forms smaller secondary vortices (Fig. 2b). The bottom vortex becomes larger and shifts slightly downstream where it decreases in strength as it begins to entrain vorticity of opposite sign by drawing the top vortex across the wake (Fig. 2c). The top vortex continues to increase in strength, occupying practically the entire breadth of the wake (Fig. 2d). The bottom vortex is still connected to the bottom separation point by a feeding shear layer. When the strengthened top vortex begins to draw the bottom shear layer across the wake, the bottom vortex downstream is no longer being fed vorticity from the separation point and is shed (Fig. 2e). The top vortex, now drawing the bottom shear layer across the wake, decreases in strength and shifts downstream while the bottom shear layer simultaneously forms a new bottom vortex. The new bottom vortex grows until it occupies most of the breadth of the wake and finally draws the top shear layer across the wake cutting off further supply of vorticity to the top vortex. The top vortex is then shed and the cycle begins to repeat. Figure 2f shows a cluster of vorticity which is the shed bottom vortex farthest downstream and a cluster which represents the top shed vortex close to the center of the plot. At high Reynolds numbers, a Karman vortex street is not observed although periodic shedding does occur.[17] Thus, an identifiable vortex structure should not appear downstream but should appear, as pointed out by Abernathy and Kronauer,[8] as a cluster of vorticity.

The calculated Strouhal number $S = 0.16$ is lower than the generally accepted value of $S = 0.21$. The calculation is based upon the first vortex shed at $t = 18.8$ and the second at $t = 25.0$. According to Sarpkaya's[16] experimental results, the second vortex is captured more rapidly than the first and subsequent vortices are captured more rapidly than the second.

Separation Angle

Figure 3 shows the variation of separation angle with time. For $t \leq 4.0$ the unsteady momentum-integral equations are solved; for $t > 4.0$ quasi-steady flow is assumed and a solution

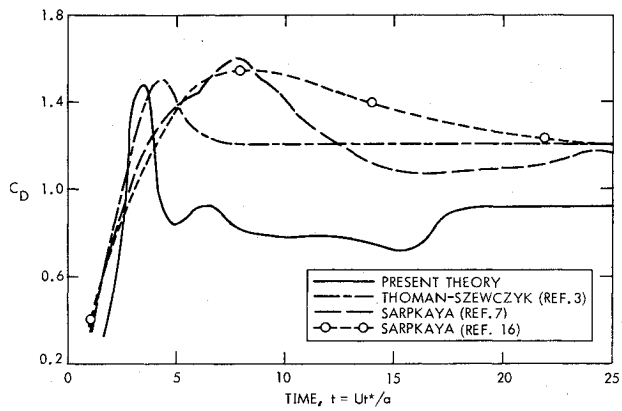

Fig. 4 Time dependent drag.

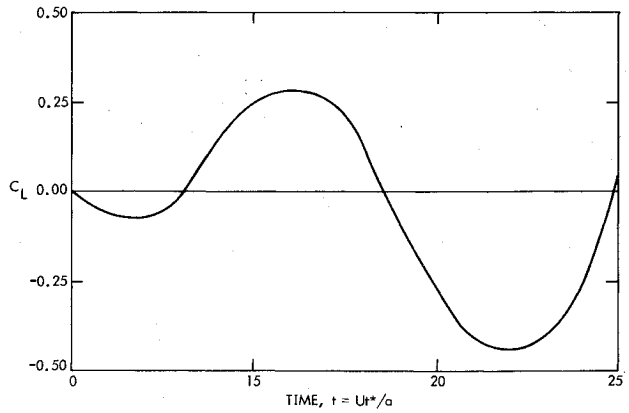

Fig. 5 Oscillating lift.

to the steady momentum-integral equations is obtained. Pohlhausen[11] velocity profiles are assumed in both cases. Figure 3a compares the current results with the work of Collins and Dennis,[18] Thoman and Szewczyk,[3] and Schuh.[10] Collins and Dennis developed a power series solution by a method of successive approximation to the Navier-Stokes equations. Thoman and Szewczyk solved the Navier-Stokes equations using finite differences. The separation points in both of these methods are obtained by noting the zero shear position from the vorticity distributions around the cylinder. Separation is similarly determined by Schuh and in the current method where the boundary-layer approximation is used and $\omega = (-\partial u/\partial y)$. The results shown in Fig. 3a are in close agreement with Collins and Dennis, and Thoman and Szewczyk. Schuh assumed a constant outer potential flow $u_o^o = 2 \sin \theta$ and obtained a final steady separation angle $\theta_s = 107.2°$. The difference between the current results and Schuh's is primarily due to the time dependent outer flow solution.

At $t = 4.0$, θ_s, as calculated by the unsteady integral momentum solution, approaches a steady value of approximately $\theta_s = 81°$ which is in good agreement with the generally accepted value of $\theta_s = 82°$ for steady flow. For longer times where quasi-steady flow is assumed, Pohlhausen's solution to the steady momentum-integral equations yields a final average value of $\theta_s = 67°$ (Fig. 3b). The asymmetry of the flow is indicated by the displacement of the top and bottom separation angles.

The discontinuity in the curve at $t = 4.0$ indicates that the error in separation angle due to the quasi-steady flow assumption is only about 5%. However, the final value of separation angle, $\theta_s = 67°$, is almost 20% lower than the usual $\theta_s = 82°$. The difficulty lies in the influence the newly created vortices have on the separation point. It was found that the separation point velocity is strongly influenced by vortices in its immediate vicinity and that the effect was to promote separation. Thus, the separation angle is continually forced toward the forward stagnation point until the favorable pressure gradient over the forward part of the cylinder balances the effect of the newly introduced vortices; hence $\theta_s = 67°$. To obtain a better estimate of separation, it will be necessary to modify the vortex birth algorithm such that the newly created vortices do not dominate the outer flow near separation.

Lift and Drag

The drag as a function of time and curves obtained by various other investigators is plotted in Fig. 4. The drag predicted by the current method is due to pressure only. A finite-difference solution to the boundary-layer equations shows that the drag due to viscous stress is negligible ($C_{ds} = 0.02$) in comparison to the pressure drag; Thom[19] shows that for the range of Reynolds numbers considered, $C_{ds} = 0.04$. The peak drag agrees well with Thoman and Szewczyk[3] and Sarpkaya.[7] After the first vortex is shed at $t \sim 16$, however, the drag approaches a quasi-steady value of $C_D \sim 0.9$, which is well below the generally accepted value of $C_D = 1.2$.

Because the steady separation angle predicted using Pohlhausen's method is only 67°, it is not surprising that the steady drag value is in error. The location at which point vortices are introduced into the wake is an important factor in the time development of the wake, and, as a result, in the time development of the drag. To determine whether a more accurate prediction of steady separation angle could improve the drag estimates, a test case was run where the motion of the separation angle was stopped at 82°. For this test case, the drag was found to approach a steady value of $C_D = 1.2$.

Oscillating lift on the cylinder occurs as a result of the alternate vortex shedding (Fig. 5). The current theory gives a peak value of approximately $C_L \sim 0.45$. Gerrard[20] and Keefe[21] experimentally obtained values of $(\bar{C}_L{}^2)^{1/2} \sim 0.5$ and $(\bar{C}_L{}^2)^{1/2} \sim 0.7$, respectively.

Conclusions

The current solution to the cylinder problem is a more phenomenological approach than finite-difference solutions. No grids or meshes of any type are required. The boundary-layer discrete vortex wake interaction provides a step-by-step account of the initial formation of the symmetric vortices behind the cylinder, their asymmetric development, and eventual alternate shedding. This approach increases computer efficiency and contributes to the physical understanding of the flow phenomena.

For the early phases of the flow ($0 < t \leq 4$), drag coefficients were obtained which fall within the range obtained by other investigators and the transient motion of the separation angle was in excellent agreement with that predicted by finite difference solution. For times greater than $t = 4.0$, it was assumed that the boundary layer responded with no time lag to changes in the outer potential flow; Pohlhausen's solution to the steady momentum-integral equations was used to predict separation. The strong influence on the outer flow velocity at separation by the point vortices nearest separation resulted in a final steady separation angle of $\theta_s = 67°$. The poor prediction of separation resulted in a steady drag value which was also low, $C_D \sim 0.9$. Oscillating values of lift which accompany the periodic shedding compare well with experiment. The postulated rear shear layer accounts for secondary vortices and for the reduction in strength of the main vortex structure. The accuracy of this method can be improved by improving the prediction of separation angle for late times. Further work is needed to correctly model the effects of the vortices nearest separation on the outer flow velocity at separation.

References

[1] Payne, R. B., "Calculations of Unsteady Viscous Flow Past a Circular Cylinder," *Journal of Fluid Mechanics*, Vol. 4, May 1958, pp. 81-86.

[2]Kawaguti, M. and Jain, P., "Numerical Study of a Viscous Fluid Past a Circular Cylinder," University of Wisconsin Math Research Center, Madison, Wisc., Rept. 590, 1965.

[3]Thoman, D. C. and Szewczyk, A. A., "Time Dependent Viscous Flow Over a Circular Cylinder," *Physics of Fluids Supplement,* (II-76, II-86), Dec. 1969.

[4]Mello, J. F., "Investigation of Normal Force Distribution and Wake Vortex Characteristics of Bodies of Revolution at Supersonic Speeds," *Journal of the Aeronautical Science*, Vol. 26, March 1959, pp. 155-168.

[5]Bryson, A. E., "Symmetric Vortex Separation on Circular Cylinders and Cones," *Journal of Applied Mechanics*, Vol. 26, Dec. 1959, pp. 643-648.

[6]Gerrard, J. H., "Numerical Computation of the Magnitude and Frequency of the Lift on a Circular Cylinder," *Philosophical Transactions of the Royal Society of London*, London Series A, Vol. 261, Jan. 1967, pp. 137-162.

[7]Sarpkaya, T., "An Analytical Study of Separated Flow about Circular Cylinders," *Journal of Basic Engineering*, Vol. 90, Dec. 1968, pp. 511-520.

[8]Abernathy, F. H. and Kronauer, R. E., "Formation of Vortex Sheets," *Journal of Fluid Mechanics*, Vol. 13, May 1962, pp. 97-106.

[9]Milne-Thomson, L. M., *Theoretical Hydrodynamics*, Macmillan, New York, 1960, Chap. 7, p. 154.

[10]Schuh, H., "Calculation of Unsteady Boundary Layers in Two-Dimensional Laminar Flow," *Zeitschrift Flugwissenschaften*, 5 Heft, 1953, pp. 122-131.

[11]Schlichting, H., *Boundary Layer Theory*, 6th ed., McGraw Hill, New York, 1968, pp. 192-197.

[12]Chorin, A. J. and Bernard, P. S., "Discretization of a Vortex Sheet, With an Example of Roll-Up," *Journal of Computational Physics*, Vol. 13, Nov. 1973, pp. 423-429.

[13]Bloom, A. M. and Jen, H., "Roll-up of Aircraft Trailing Vortices Using Artifical Viscosity," *Journal of Aircraft*, Vol. 11, Nov. 1975, pp. 714-716.

[14]Lamb, H., *Hydrodynamics*, Dover, New York, 1945, 6th ed., Chap. 7, pp. 214-215.

[15]Gerrard, J. H., "An Experimental Investigation of the Oscillating Lift and Drag of a Circular Cylinder Shedding Turbulent Vortices," *Journal of Fluid Mechanics*, Vol. 11, Sept. 1961, pp. 244-245.

[16]Sarpkaya, T., "Separated Flow About Lifting Bodies and Impulsive Flow About Cylinders," *AIAA Journal*, Vol. 4, March 1966, pp. 414-420.

[17]Morkovin, M. V., "Flow Around Circular Cylinder-A Kaleidoscope of Challenging Fluid Phenomena," *ASME Symposium on Fully Separated Flows*, Arthur G. Hansen, ed., May 18-20, 1964, pp. 102-118.

[18]Collins, W. M. and Dennis, S. C. R., "The Initial Flow Past an Impulsively Started Circular Cylinder," *Quarterly Journal of Mechanics and Applied Mathematics*, Vol. 26, Feb. 1973, pp. 53-75.

[19]Rosenhead, L., ed., *Laminar Boundary Layers*, Oxford University Press, 1963, Chap. 2, p. 106.

[20]Gerrard, J. H., "The Calculation of the Fluctuating Lift on a Circular Cylinder and its Application to the Determination of Aerolian Tone Intensity," AGARDograph 463, April 1963.

[21]Keefe, R. T., "An Investigation of the Fluctuating Forces Acting on a Stationary Cylinder in a Subsonic Stream and of the Associated Sound Field," *Acoustical Society of American Journal*, Vol. 34, Nov. 1962, pp. 1711-1714.